American Mineralogist, Volume 69, pages 531–540, 1984

Magnesium staurolite and green chromian staurolite from Fiordland, New Zealand

C. M. WARD

Department of Geology,
University of Otago, Dunedin, New Zealand

Abstract

Staurolite with up to 6.5% MgO and magnesium as the dominant divalent cation is recorded from an incompletely reconstituted metatroctolite from Fiordland, New Zealand. It occurs in complex assemblages including pyrope, hornblende, spinel and corundum, and is estimated to have crystallized at about 12 kbar and 750°C. The *a* cell edge of this staurolite (7.891Å) is markedly larger than that of other natural staurolites, which may be attributed to substantial substitution of Mg for Al in the "kyanite" layer of the staurolite structure.

A green staurolite with 2% Cr_2O_3 is also recorded from a mafic metatuff from Fiordland.

Introduction

In their thorough review of staurolite crystal chemistry, Griffen and Ribbe (1973) noted that staurolite exhibits "remarkable chemical constancy for a mineral so chemically and structurally complex". This relative constancy is at least in part due to the rather narrow range of metamorphic conditions and bulk rock compositions in which staurolite has generally been observed—typically in moderately high grade pelites. Several features of its chemistry hint at the wide range of staurolite compositions possible in different bulk compositions metamorphosed under appropriate conditions. The affinity of staurolite for zinc, with ZnO contents commonly up to 2% (e.g., Guidotti, 1970) and occasionally 7.5% (Juurinen, 1956), is well known, and Griffen (1981) has recently synthesized pure Zn-staurolite. Blue cobalt staurolite or "lusakite" with 8.5% CoO associated with cordierite–anthophyllite gneiss has been described from Zambia (Skerl and Bannister, 1934). Gibson (1978) has described an occurrence of staurolite in sheets of amphibolite and hornblendite in a metamorphosed layered basic intrusion in central Fiordland, New Zealand. The staurolite is unusually low in iron, compensated by higher magnesium and aluminum contents. Hellman and Green (1979) have experimentally produced magnesium staurolite (Mg > Fe) from tholeiitic compositions at high pressure, and Schreyer and Seifert (1969) synthesized iron-free Mg-staurolite.

During investigation of a complex polymetamorphic terrane in the Dusky Sound area of Fiordland, 20–40 km southwest of the localities described by Gibson (1978), staurolite has been observed in a wide variety of rock types. In addition to typical low pressure pelites with andalusite and higher pressure pelites with kyanite and garnet, staurolite host rocks include metagabbro, metatroctolite, probable mafic metatuffs, and a metabasalt dike. These metabasites are geologically independent of each other, and of the body described by Gibson (1978). In many of these rocks the staurolite is present in very minor quantities (<0.1 modal percent), is fine grained and often paler than usual. It seems likely that staurolite is more widespread in metabasites than the present meager record would suggest.

Many staurolites from the Fiordland metabasites have compositions differing only subtly or not at all from those of pelitic staurolites. However this paper presents data on two extreme varieties found in metabasites of the Dusky Sound area, being the first records of natural staurolite with magnesium as the dominant divalent cation, and of green, chromian staurolite.

Nomenclature

"Magnesium staurolite" is used in this paper to denote staurolite with magnesium cations in excess of all others except aluminum and silicon (where all iron is combined as Fe^{2+}). "Magnesian", "chromian" etc. imply unusually large, though still subordinate magnesium, chromium etc. contents. Magnesium staurolite should not necessarily be regarded as a new end-member mineral species analogous to iron staurolite in which Fe is the dominant (divalent) cation, since Fe and Mg may occupy different sites in the structure (Smith, 1968; Griffen and Ribbe, 1973; and see below).

"Lusakite" (Skerl and Bannister, 1934) is a cobalt staurolite with Co > total Fe > Mg, the only silicate mineral with a substantial cobalt content. It has not in the past been accepted as a valid mineral species, perhaps because of a misconception of the actual composition; thus Fleischer (1980) quotes the formula as $(Fe^{2+}, Mg,Co)_2Al_9Si_4O_{23}(OH)$, implying that Fe > Mg > Co.

0003–004X/84/0506–0531$02.00

Recently Čech et al. (1981) have reasserted the claim of "lusakite" to be a valid species on the grounds that cobalt is the dominant cation. However, it must be presumed that the crystal chemistry of Co in staurolite is as complex as that of Fe and Mg. In the absence of definitive data on the distribution of the Co, the non-commital term "cobalt staurolite" is more appropriate.

Analytical methods

Mineral analyses were made with the University of Otago's JEOL JXA-5A electron microprobe, an automated crystal spectrometer machine, using a variety of natural and synthetic oxides and silicates as standards. The data were corrected on-line by the method of Bence and Albee (1968). Six 5-second counts were integrated for each element analysis. Greater precision was obtained for some trace elements (Zn, Mn in Table 1 staurolites; V, Cu in Table 3 staurolites) by integrating ten 10-second counts on peak and background. Vanadium analyses were corrected for interference from Ti$K\beta$. Tabulated analyses are the means of 2–4 similar analyses, usually on the same grain.

Magnesium staurolite

Magnesium staurolite was found in specimen OU 48255, a partially metamorphosed ultrabasic rock which was probably a hornblende olivine gabbronorite (Streckeisen, 1976) prior to metamorphism. For the sake of brevity, and to emphasize the role of igneous olivine and plagioclase as the major reactants responsible for the metamorphic assemblages in the rock, it is hereafter referred to as a metatroctolite. The specimen is a pebble collected from float in a small stream draining amphibolite-facies metasediments and dioritic orthogneiss north of Dusky Sound. It is tentatively inferred that it was derived from a xenolith in the orthogneiss.

The igneous mineralogy of the specimen has been largely reconstituted by extension of irregular metamorphic coronas between olivine or orthopyroxene and plagioclase to encompass most of the rock. Staurolite is patchily distributed in trace quantities as two types, designated 1 and 2, which are distinguished primarily on the basis of their local parageneses, and secondarily on the basis of their compositions (Table 1). Type 1 staurolite, with *Mg* about 45, occurs with hornblende and pleonaste spinel (±corundum, ±clinozoisite, ±anorthite). Type 2 staurolite, with *Mg* about 55, occurs with garnet and more magnesian hornblende. Both types of staurolite are exceptionally magnesian, with about 5% and 6% MgO respectively, compared with the normal range of 1–3%.

Petrography

Specimen OU 48255 is heterogeneous on a scale of a few millimeters, partly because of initial (igneous) heterogeneity on this scale, and partly because of the variable

Table 1. Microprobe analyses of staurolite from metatroctolite OU 48255

	Type 1			Type 2		
	1	2	3	4	5	6
SiO_2	26.88	27.40	27.39	27.19	27.75	27.42
Al_2O_3	53.98	53.99	54.37	56.16	54.77	54.66
Cr_2O_3	0.00	0.01	0.01	0.01	0.02	0.02
CaO	0.07	0.03	0.15	0.02	0.04	0.02
MnO	0.15	0.19	0.15	0.04	0.07	0.03
MgO	5.05	5.11	5.22	5.61	6.27	6.48
FeO	11.86	11.07	10.94	8.30	8.74	9.31
ZnO	0.05	0.06	0.00	0.13	0.02	0.03
TiO_2	0.07	0.14	0.10	0.34	0.17	0.23
	98.10	98.00	98.33	97.80	97.84	98.20
	Cations per 46 oxygens					
Si	7.406	7.521	7.488	7.374	7.538	7.448
Al	17.526	17.467	17.516	17.948	17.531	17.499
Cr	0.000	0.003	0.001	0.001	0.005	0.004
Ca	0.020	0.010	0.043	0.006	0.011	0.006
Mn	0.034	0.044	0.034	0.009	0.015	0.007
Mg	2.073	2.092	2.127	2.269	2.537	2.622
Fe	2.733	2.542	2.502	1.882	1.986	2.115
Zn	0.009	0.010	0.000	0.026	0.004	0.006
Ti	0.015	0.029	0.021	0.068	0.034	0.048
	29.82	29.72	29.73	29.58	29.66	29.75
*Mg**	43.1	45.1	45.9	54.7	56.1	55.4

Unit cell dimensions, Type 2 (Å): *a* 7.891(3); *b* 16.617(5); *c* 5.658(2)

* 100 Mg/(Mg + Fe)

nature and extent of the metamorphic reactions which have incompletely reconstituted the rock. Olivine (Fo_{79}), orthopyroxene (En_{80}), clinopyroxene ($Wo_{45}En_{48}Fs_7$, 5% Al_2O_3), plagioclase (An_{79-82}) and poikilitic hornblende are present as igneous relics in minor amounts, generally no more than a few percent each, though locally dominant. The olivine is surrounded by extensive coalescing coronas consisting of orthopyroxene (locally with symplectic intergrowths of magnetite), followed by pale green hornblende then a symplectic intergrowth of fine vermicular green spinel (pleonaste) within coarse irregular hornblende. In more thoroughly reconstituted patches olivine and igneous pyroxenes are lacking, metamorphic orthopyroxene and hornblende are dominant, with prominent spinel both in symplectite with hornblende and less commonly in a fine granular mosaic. Dolomite and magnetite may also be present. Relict igneous plagioclase is rimmed by anorthite (An_{94-99}) often accompanied by clinozoisite (and zoisite?). Hornblende–spinel encloses plagioclase but spinel may be absent within a few hundred microns of the plagioclase, very thin plates of corundum (<300 × 3–5 μm) or fine prisms of type 1 staurolite being present instead (Fig. 1a). The corundum, staurolite and

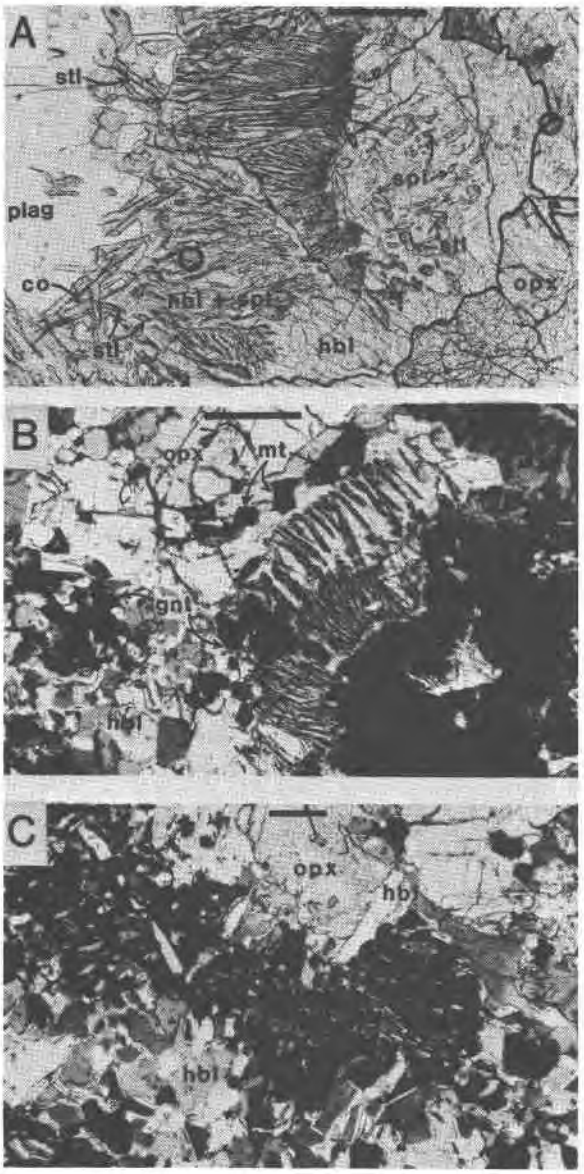

Fig. 1. Metamorphic textures in metatroctolite OU 48255. See Fig. 2 for mineral abbreviations. Scale bar 0.2 mm in each photomicrograph. (a) Reaction zone between orthopyroxene (heavily outlined at right) and plagioclase. Spinel, staurolite and corundum occur as fine inclusions in coarse hornblende. Plane polarized light. (b) Two textural variants of hornblende–spinel symplectite (center) partially replaced by garnet (center and right). Garnet and granoblastic hornblende to left. Crossed polarizers. (c) Garnet (right-center to upper left) with stumpy staurolite inclusions at upper left and slender corundum inclusions right-center. Crossed polarizers.

spinel grains may show a crude zonation away from plagioclase towards orthopyroxene in the above order or occur mixed in pairs, all as dispersed grains within a "background" of hornblende.

Garnet was produced by a further reaction affecting substantial domains interpenetrating with the garnet-free domains. Garnet clearly replaces hornblende-spinel symplectites (Fig. 1b); additional orthopyroxene appears to be consumed also. Extensive aggregates of equigranular polygonal hornblende generally lie adjacent to the garnet. This hornblende is significantly more magnesian than that remote from garnet (see below and Table 2); it has clearly recrystallized in response to growth of the garnet. Chlorite is an infrequent associate of this assemblage but is not found in garnet-free domains. Small irregular inclusions of relict spinel or hornblende are common but not ubiquitous in garnet. Semi-radiating sprays of platy corundum may be present instead, and rarely, granular corundum occurs with hornblende adjacent to garnet. A few subhedral staurolite prisms ($<200 \times 50$ μm), designated type 2 also occur as inclusions in garnet (Fig. 1c) or as separate adjacent grains.

Table 2. Microprobe analyses of minerals in metatroctolite, OU 48255

	1 hbl	2 hbl	3 spl	4 gnt	5 gnt	6 gnt	7 chl	8 opx	9 czo
SiO_2	44.17	44.92	0.17	40.69	40.33	40.02	27.97	53.58	39.15
Al_2O_3	17.39	14.51	64.33	23.12	22.92	22.41	22.61	3.15	31.15
TiO_2	0.06	0.14	0	0.02	0.02	0.03	0.02	0.03	0.07
*Fe_2O_3			1.02						3.20
FeO	7.96	6.57	19.84	17.84	18.77	17.05	5.33	14.82	0.88
MnO	0.13	0.05	0.10	0.57	0.61	0.46	0	0.31	0.10
MgO	14.00	17.05	14.62	14.58	12.30	12.20	30.28	28.06	0.15
CaO	12.16	12.03	0.08	4.06	5.74	7.44	0.01	0.20	23.34
Na_2O	1.63	1.98	0	0.02	0.03	0	0.03	0	0.02
K_2O	0.04	0.05	0	0.01	0	0	0	0.01	0
Cr_2O_3	0.01	0	0.03	0.01	0.02	0.01	0.01	0.03	0
ZnO	-	-	0.07	-	-	-	-	-	-
	97.55	97.30	100.26	100.92	100.73	99.61	86.26	100.20	98.05
				Mineral Formulae					
Si	6.293	6.397	0.009	5.962	5.976	5.984	5.380	1.919	2.999
Al	2.920	2.436	3.942	3.992	4.002	3.949	5.125	0.133	2.813
Ti	0.007	0.015	0	0.002	0.003	0.003	0.004	0.001	0.004
*Fe^{3+}			0.040						0.184
Fe^{2+}	0.949	0.783	0.863	2.186	2.327	2.132	0.857	0.444	0.057
Mn	0.015	0.007	0.005	0.070	0.076	0.058	0	0.009	0.007
Mg	2.973	3.620	1.136	3.184	2.717	2.720	8.681	1.498	0.017
Ca	1.856	1.836	0.005	0.638	0.911	1.191	0.002	0.008	1.916
Na	0.450	0.545	0	0.006	0.009	0	0.012	0	0.004
K	0.006	0.009	0	0.002	0	0	0	0	0
Cr	0.001	0	0.001	0.001	0.002	0.001	0.001	0.001	0
Zn	-	-	0.003	-	-	-		-	-
	15.468	15.647	6.002	16.043	16.023	16.038	20.060	4.013	8.000
(O)	23	23	8	24	24	24	28	6	12
Mg	75.8	82.2	56.8	59.2	53.9	56.1	91.0	77.1	-
		pyrope		52.4	45.1	44.6			
		almandine		36.0	38.6	34.9			
		grossular		10.5	15.1	19.5			
		spessartine		1.2	1.3	1.0			

* *Iron distributed between Fe_2O_3 and FeO according to stoichiometry in spinel and clinozoisite. All iron as FeO in other minerals.*

1, hornblende adjacent to spinel and type 1 staurolite
2, hornblende adjacent to garnet
3, spinel adjacent to hornblende 1 and type 1 staurolite
4, garnet core 5, garnet adjacent to type 2 staurolite
6, garnet rim 7, chlorite
8, metamorphic orthopyroxene 9, clinozoisite

Mineral chemistry

The patchiness of the two groups of assemblages (i.e., those with and without garnet) on a millimeter scale implies a very limited range of diffusion and equilibration. This impression is supported by the mineral chemistry. The equilibration of garnet with type 2 staurolite but not type 1 is demonstrated by the consistently lower Mn and Fe contents of type 2 staurolites (Table 1) and their higher *Mg* noted above. Other variations in staurolite chemistry probably reflect local variation in the chemical potentials of some components. Thus staurolite 4, with significantly higher Al and lower (Mg+Fe) contents than the other staurolites, is an inclusion in garnet which (atypically) impinges on plagioclase, the primary source of the alumina in the metamorphic system. Staurolite 3, with a significant trace of calcium, is in contact with clinozoisite. (The CaO content was consistent in multiple analyses and is not an artifact of the edge effect.) The titanium content is variable and low (cf. Griffen and Ribbe, 1973) reflecting the low bulk rock titanium content—primary hornblende with less than 1% TiO_2 is the only significant source of titanium.

Hornblende analyses 1 and 2 (Table 2) are analogous to types 1 and 2 staurolite. The lower Mn content and higher *Mg* ratio of hornblende 2 again relate to equilibration with garnet. The sodium content of hornblende, though modest, is only slightly lower than that of the very small quantity of surviving igneous plagioclase ($\sim An_{80}$) and considerably higher than that of metamorphic plagioclase ($\sim An_{98}$), hence the majority of the sodium in the system is in hornblende. The higher sodium content of hornblende 2 relative to hornblende 1 is thus interpreted as a consequence of the reduced modal hornblende after crystallization of garnet.

Garnet is zoned and pyrope-dominant (Table 2). Garnet 5 enclosing staurolite has a lower *Mg* than the others, such that the usual relationship that garnet has a slightly lower *Mg* than coexisting staurolite (Albee, 1972) is retained. The higher almandine component in this garnet suggests that staurolite may be restricted to domains slightly richer in iron. The marked enrichment in the grossular component from core to rim (garnets 4–6, Table 2) is perhaps a reflection of increasing pressure during crystallization.

A feature of the clinozoisite composition is the apparent substitution of (Fe^{2+} + Mg + Mn) for about 4% of the Ca atoms.

Reaction relationships

Two sequential groups of metamorphic assemblages are established on the basis of the petrography and mineral chemistry, garnet and chlorite being restricted to the second group. Suggested reactions are as follows:

orthopyroxene + plagioclase + H_2O
→ hornblende(1) + (spinel, staurolite, corundum)
+ anorthite (±clinozoisite) (1)

and subsequently

hornblende(1) + spinel + orthopyroxene
→ hornblende(2) + garnet ±chlorite (2a)

and hornblende(1) + spinel + orthopyroxene
→ hornblende(2) + garnet + (corundum,staurolite). (2b)

Rigorous chemographic analysis of these reactions in a multicomponent silica-deficient system would be difficult if not impossible. There are no suitable phases from which to project the important minerals onto a 3- or 4-component system. In practice, simple ACF diagrams were found to be useful. This involves the assumption, among others, that silica is sufficiently mobile that spatial variation in silica activity is not a significant factor limiting the assemblages. In this way, the essential features of the two groups of reactions are shown in Figure 2, where the somewhat variable mineral compositions are represented by points. The "difficulties" caused by silica are relatively minor, for example consideration of the silica balance of reaction 1 suggests that a silica-poor phase is required as a reactant. Presumably this is magnetite, to account for the lower *Mg* ratio of (hornblende + spinel) relative to orthopyroxene, and the significant quantity of Fe^{3+}-bearing clinozoisite produced. Reaction 1 thus becomes

orthopyroxene + plagioclase + magnetite + H_2O
→ hornblende + (spinel, staurolite, corundum)
+ anorthite + clinozoisite

Metamorphic conditions

The formation of pyrope garnet and magnesium staurolite implies a high pressure of metamorphism. Schreyer and Seifert (1969) synthesized Mg-staurolite in an iron-free system at high pressures and temperatures, but could

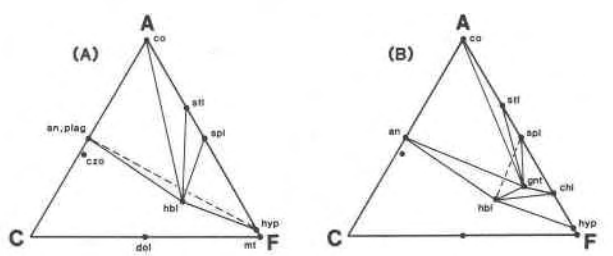

Fig. 2. ACF diagrams illustrating the assemblages and reaction relationships in OU 48255. A is molecular Al_2O_3–Na_2O–K_2O, C is CaO, and F is FeO + MgO. Mineral abbreviations: an - anorthite; plag - plagioclase; czo - clinozoisite; dol - dolomite; hbl - hornblende; mt - magnetite; hyp - hypersthene; spl - spinel; stl - staurolite; co - corundum; gnt - garnet; chl - chlorite; (A) represents the first group of reactions, basically the breakdown of hypersthene + plagioclase; and (B) represents the subsequent reactions, basically the breakdown of hornblende (1) + spinel, but note that hornblende (2) persists with staurolite and corundum.

not find a stability field below 12 kbar and 800°C. In contrast Fe-staurolite is stable to pressures as low as 1 kbar (Richardson, 1968), implying that the Mg content of staurolite in Mg–Fe systems will be strongly pressure dependent. This is corroborated by the experimental production of staurolite with *Mg* 54–57 in model tholeiite compositions at about 750° and 25 kbar water pressure by Hellman and Green (1979). Under these conditions the staurolite *Mg* approaches that of the bulk rock, 70.

More precise assessment of the metamorphic conditions affecting this complex natural system, which includes mixed volatiles as indicated by the presence of both hydrous and carbonate minerals, is a difficult problem. The limited range of equilibration and the metastable persistence of substantial volumes of igneous relics and early metamorphic assemblages, suggestive of fluid-deficient conditions, are further complicating factors. The uncertain origin of the metatroctolite specimen precludes the use of assemblages in adjacent rocks to assist in determination of the metamorphic conditions.

In a pioneering study Obata and Thompson (1981) analyzed reaction topologies in the model mafic-ultramafic system $CaO–MgO–Al_2O_3–SiO_2–H_2O$, calibrated against the limited experimental data. Their reaction 26 (hornblende + orthopyroxene + spinel + anorthite = garnet + chlorite) is closely analogous to reaction 2a. This reaction is "water conserving" hence essentially independent of $a(H_2O)$, and is predicted to occur at 11–13 kbar and 700–800°C. The effect of iron on the system, and the changed topology with the addition of phases not considered by Obata and Thompson such as clinozoisite and staurolite, are undoubtedly important. Nevertheless these figures are a useful starting point for an estimate of the *P–T* conditions responsible for the formation of magnesium staurolite in the metatroctolite.

Some indication of the temperature of metamorphism is given by Fe–Mg partitioning between adjoining clinopyroxene and orthopyroxene rims. Clinopyroxene, which is considered to be entirely of relict igneous origin, shows extensive exsolution of fine hornblende lamellae (cf. Yamaguchi et al., 1978). A thin rim (~30 μm) is generally free of these lamellae and markedly depleted in Al_2O_3 (2% cf. 5%). The rim is interpreted to have metastably equilibrated with the immediately adjacent phases. Two-pyroxene temperatures for these materials calculated after Wells (1977) are reasonably consistent at 760°C (±30). Although this estimate is compatible with that derived from the phase relations of Obata and Thompson (1981), it must be treated with caution since it is unclear when the pyroxene rims were last able to equilibrate relative to the timing of the metamorphic reactions.

Schreyer (1967) suggested that the lack of natural magnesium staurolite was due to the absence of very aluminous, magnesian bulk compositions metamorphosed at sufficiently high pressure. In a sense the present exceptional staurolite reinforces this view. It is involved in only local equilibrium with other aluminous phases, while a substantial proportion of relict pyroxene and olivine remains. If the rock had been fully reconstituted the staurolite is unlikely to have survived. For magnesium staurolite to form in more typical basic compositions, presumably much higher pressures are required, tending towards the 24–26 kbar used by Hellman and Green (1979) to crystallize magnesium staurolite in model tholeiite compositions.

Staurolite crystal chemistry

Idealized formulae such as $(Fe,Mg)_4Al_{18}Si_{7.5}O_{44}(OH)_4$, $(Fe,Mg)_4Al_{17.33}Si_8O_{44}(OH)_4$, or $(Fe,Mg)_4Al_{18}Si_8O_{46}(OH)_2$ misrepresent the complex crystal chemistry of staurolite (Smith, 1968). Griffen and Ribbe (1973) inferred from a statistical study of staurolite analyses that Fe, Mg and Al are each distributed over both the tetrahedral Fe site and the octahedral Al sites, with Fe preferring the former and Mg and Al the latter. Thus Fe and Mg are not related by the simple one-for-one substitution scheme implied by the formulae above. The present analyses were normalized on a 46-oxygen basis, equivalent to assuming 4H per formula unit. On this basis the total of Mg + Fe cations is unusually high, up to 4.81, compared with a maximum of 4.47 and mean 4.07 for the 18 staurolites with less than 1% ZnO analysed by Griffen and Ribbe (1973). This feature is also manifested by unusually high cation totals, 29.58 to 29.82 (cf 29.33 to 29.55, mean 29.43 recorded by Griffen and Ribbe).

Figure 3 explores relations between Mg + Fe and Al cell contents with plots of Mg + Fe against Al, and against Al′, where Al′ is Al + Si−8 (that is, Al cations per unit cell after subtacting sufficient Al to make up the occupancy of the Si site to 8). The markedly improved correlation after this adjustment is obvious, and this is

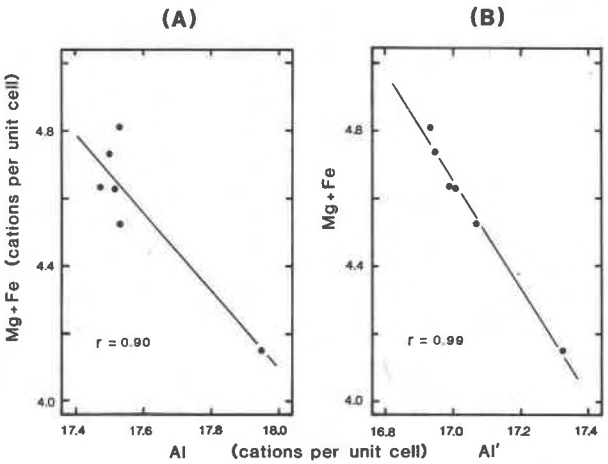

Fig. 3. (A) Mg + Fe against Al, and (B), Mg + Fe against Al′ (= Al+Si − 8) for staurolite from metatroctolite OU 48255. Least squares regression lines are shown. In (A) the regression is entirely controlled by the most aluminous staurolite. Slope of the regression line in (B) is −1.59.

strong support for the common assumption that it is Al which makes up the Si site to essentially full occupancy (Smith, 1968; see also Griffen et al., 1982). The extent of the adjustment is considerable because of the variable and low Si content of the unit cells. The low Si content is presumably a manifestation of the low silica activity of the rock, indicated by the absence of quartz and the abundance of spinel with minor corundum.

The very good negative correlation of Mg + Fe against Al′ (despite considerable variation of *Mg*) supports Griffen and Ribbe's (1973) deduction of an important (Mg,Fe)⇌Al substitution which they inferred to take place mainly in the octahedral sites. The slope of the regression line is close to −1.5, the figure to be expected for the simple substitution 3(Mg,Fe)⇌2Al.

Cell dimensions

Griffen and Ribbe (1973) plotted staurolite unit cell dimensions against iron content, and demonstrated that *a* was insensitive to iron content while *b*, and to a lesser extent *c*, both increase with increasing iron. These results were interpreted in terms of the structure (Smith, 1968), which has a monolayer with the approximate composition $Fe_2Al_{0.7}O_2(OH)_2$ (the "iron" layer, see Fig. 4) lying parallel to (010), alternating with slabs of Al_2SiO_5 composition and kyanite structure. Since Fe^{2+} is the largest significant cation in staurolite and assuming that all or most of the cation substitution takes place in the iron layer, increasing Fe content causes expansion of the thickness of the iron layer thus increasing *b*. In the *a* direction the Fe tetrahedra are flanked by only slightly occupied U octahedra which are readily deformed, hence *a* does not increase. The Fe tetrahedra are linked by Al(3) octahedra to form a zig-zag chain parallel to *c*, hence the expansion of *c* with increasing iron content. Because of the indirectness of this linkage, and the geometric integrity of the adjoining kyanite layers, the increase in *c* is small.

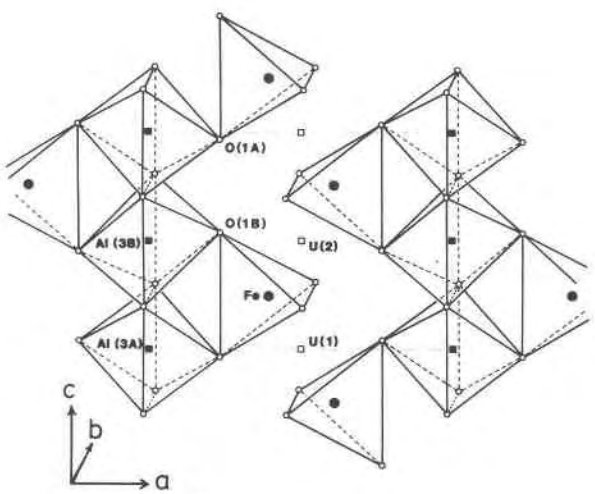

Fig. 4. The "iron" layer of staurolite, cf. Dickson and Smith (1976) and Ribbe (1980). (Note however the distortion of these authors' diagrams due to assumption that *c*/*a* is 0.5 rather than 0.70) The unit cell boundaries are shown by the dotted lines.

Griffen et al. (1982) have recently refined this analysis by plotting cell dimensions against mean ionic radius of the cations inferred to occupy the iron layer, to allow for the effect of deviations from simple Fe,Mg chemistry. All Fe, Mg and Zn are assumed to be in the iron layer, together with Al in excess of that in the kyanite layer, and cations are distributed between tetrahedral and octahedral sites according to defined rules. The cell dimensions vary according to essentially the same pattern with improved correlation coefficients, and the interpretation was reaffirmed.

Unit cell dimensions of a single crystal of type 2 staurolite, determined with the use of a Gandolfi X-ray camera, are presented in Table 1. Because of the small crystal size and slight contamination with garnet only 14 lines were available for the least squares refinement of the data. An orthorhombic cell was assumed.

Cell edges *b* and *c* of this staurolite lie close to the regression lines of cell edges against mean ionic radius calculated by Griffen et al. (1982), and within the field of other staurolites.[1] However, at 7.891Å, *a* is substantially larger than in other natural staurolites (range 7.865–7.879Å), and this is particularly notable since the variation observed in other staurolites is not significantly correlated with mean ionic radius in the iron layer. This suggests that *a* is varying in response to changes in sites in the kyanite layer.

The outstanding chemical features of this staurolite which might account for the abnormal *a* cell edge are the high Mg content and the high cation total. Figure 5 shows *a* plotted against Mg cations and against cation total for the magnesium staurolite and the 19 staurolites used by Griffen et al. (1982). There are good positive correlations in both cases, and these remain significant even if the magnesium staurolite is excluded from the regressions. On this basis it is suggested that significant substitution of Mg for Al occurs in the kyanite layer of staurolite, as was modelled by Smith (1968) in his site refinements. This effect would appear to be stronger when the cation total is higher, perhaps because of the lower number of vacancies and the resulting "competition" for sites.

The most likely site for divalent ions to substitute for Al^{3+} in the kyanite layer is Al(2), because as noted by Griffen and Ribbe (1973) this site is coordinated to the underbonded O(3) and half-hydroxyl O(1A) and O(1B). Al(2) sites are in pairs lying on either side of the iron

[1] It is assumed that the composition of the X-rayed staurolite is the mean of analyses 5 and 6 of Table 1, because it was picked from a plagioclase-free part of the specimen. It was necessary to add Mg as well as Al to the Fe site to make up the occupancy to 4 cations since the Al content of the iron layer is insufficient. The resulting mean radius is 0.603Å.

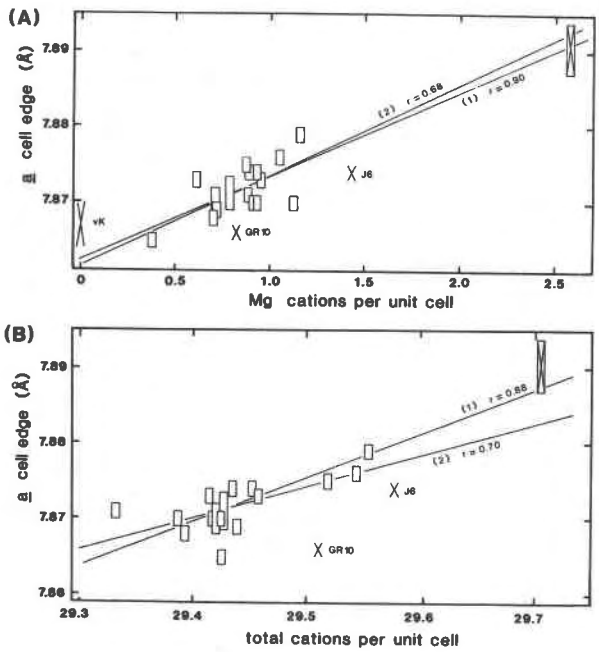

Fig. 5. (A) Staurolite *a* cell edge against Mg, and (B), *a* against cation total, for the 19 staurolites used by Griffen et al. (1982), together with that from OU 48255. Height of symbols represents ±1 e.s.d., width is arbitrary. Data points represented by crosses were not included in the regression analyses because of major deviations from (Mg,Fe) chemistry. Dual symbol at top right represents magnesium staurolite from OU 48255, which was included in regressions (1) but excluded from regressions (2). J6 = staurolite 6, Juurinen (1956) (as refined by Griffen and Ribbe, 1973), GR 10 = staurolite 10, Griffen and Ribbe, vK = von Knorring et al. (1979). J6 and GR 10 each have about 1.5 Zn cations per unit cell. From the data of Griffen (1981), their *a* cell edges would be expected to increase by about 0.007Å if this Zn was replaced by Fe, putting the points close to the calculated regression lines. It may be suggested that staurolite vK, from a shear zone in a pegmatitic crystal of amblygonite ($LiAl(PO_4)F$), owes its extreme composition (19.3 Al cations per 46 oxygens, 2.4 (Fe+Mg+Zn), cation total 29.01) to substantial substitution of Li+Al for 2(Fe, Mg, Zn).

layer, sharing the short edge O(1A)–O(1B). Substitution of larger cations in this site would readily increase *a*. In contrast *c* would not be significantly affected, because it is largely controlled by the length of continuous chains of Al(1) octahedra parallel to *c*, as is shown by the unusually short O(1A)–O(1B)–O(1A) distance (Smith, 1968). If significant Mg were to substitute for Al in the Al(1) sites, *c* would be expected to increase. This is not observed, although it might be that the contraction of *c* due to the generally decreasing Fe with increasing Mg is masking this effect. Similarly the apparent absence of any effect on *b* from the inferred substitution of considerable Mg for Al in Al(2) is readily explained by the concomitant substitution of Al for (Fe,Mg) in the Fe site.

Griffen and Ribbe (1973) note that Fe–Mg staurolites synthesized by Richardson (1966) and Fe-free Mg-staurolite synthesized by Schreyer and Seifert (1969) have *a* cell edges consistently about 0.015Å larger than the then known natural staurolites, whereas *c* is indistinguishable and *b* is perhaps a little smaller in the synthetic staurolites. These features are matched by the natural magnesium staurolite. In the light of the foregoing discussion it is suggested that to a considerable extent divalent ions are substituting for Al in the kyanite layer of the synthetic staurolites. Since the large *a* is also shown by the pure Fe-staurolite, it would seem that at least in the synthetic minerals both Fe and Mg can substitute for Al. The synthetic staurolites were all prepared at high pressure (~20 kbar), and the natural staurolite is also inferred to have formed at high pressure (~12 kbar). It seems reasonable to conclude that substitution of divalent ions for Al in the kyanite layer is promoted by high pressure, and that consequently the *a* cell edge of staurolite may be a crude pressure indicator. A larger cell edge might be expected to cause a lower density, which would be incompatible with higher pressure. However the negative effect of the cell edge on density is greatly exceeded by the positive effect of the larger cation total (Fig. 5b).

Conclusions

Staurolite from the "metatroctolite" greatly extends the range of magnesium content known from natural material, and appears to be the first record of natural magnesium staurolite. The rock is very heterogeneous and includes significant volumes of alumina-poor igneous relics, so that the local systems containing staurolite are very aluminous. Two phases of metamorphic reactions are apparent, each incomplete, leaving the rock dominated by complex reaction textures. Metamorphic conditions responsible for the crystallization of the magnesium staurolite during the second phase, perhaps of higher pressure than the first, are estimated to have been in the vicinity of 12 kbar and 750°C.

The *a* cell edge of the magnesium staurolite is markedly higher than that of other natural staurolites but comparable to that of synthetic staurolites produced at 20 kbar. It is inferred that significant substitution of Mg (and perhaps Fe) for Al takes place in the Al(2) site of the kyanite layer in staurolite, this effect being more pronounced at higher pressures. The *a* cell edge of staurolite may be useful as a crude pressure indicator.

On the basis of their crystallization of staurolite in model tholeiite compositions at 24–26 kbar, Hellman and Green (1979) suggested that staurolite may be widespread in mafic rocks metamorphosed at high pressures, as for example in subducted lithosphere. While the present occurrence of staurolite is certainly consistent with this suggestion, high pressure is evidently not a *necessary* condition for the formation of staurolites in general in metabasites. Spear (1982) has documented occurrences of

staurolite (with *Mg* 23–28 in Zn-poor crystals) in amphibolites metamorphosed at 5–6 kbar, and authigenic staurolite with *Mg* 19 occurs in a metabasite dike cutting andalusite-bearing pelites south of Dusky Sound, Fiordland (Ward, in prep.). The significance of higher pressure would appear to be principally in promoting a high *Mg* ratio in staurolite, i.e., reducing the partitioning of Fe into staurolite relative to the more magnesian minerals. Thus at lower pressures staurolite may be restricted to the more iron-rich metabasites.

Chromian staurolite

Staurolite with the unusual pleochroic scheme *X* clear, slightly bluish green, *Y* yellowish green, *Z* muddy greenish yellow, $Z > Y > X$, was observed in trace quantities in two specimens of amphibole-rich rock from north of Dusky Sound. They are from a distinctive lithostratigraphic unit generally about 20 m thick, dominated by rocks rich in amphiboles (50–99%) with no feldspar and generally little or no quartz. Aluminous minerals including garnet, chlorite, kyanite and staurolite are major phases in some streaks, pods and bands within the amphibolerich rocks. From the evidence provided by sharply defined hornblende pseudomorphs after igneous clinopyroxene, and the peripheral interbanding on a decimeter-meter scale of the amphibole-rich rocks with metasediments including pelite and metaconglomerate, it is inferred that the unit is probably a metatuff of unusual composition.

Petrography

The two rocks with "green" staurolite, OU 48093 and OU 48097, both have the assemblage gedrite–quartz–hornblende–kyanite–chlorite–rutile–phlogopite–staurolite–allanite. Magnesian chlorite, in apparent textural equilibrium with the other phases, is present as a major phase in OU 48097, but as only a trace in OU 48093.

Specimen OU 48093 is conspicuously banded with alternating quartz-rich (40–70%) and quartz-poor (2–10%) layers 2–10 mm thick. Pale green hornblende is a major phase only in some of the quartz-poor bands. These hornblende-rich bands contain all the staurolite and most of the phlogopite and allanite. Staurolite generally occurs as a minor associate of kyanite–phologopite (±quartz) pools interstitial to coarser hornblende and gedrite. It is fine-grained, with prisms typically about 50–80 μm long. On a thin section scale its modal abundance is less than 0.01%. Petrographic recognition is hindered by its similarity to allanite in the same rock, in its pleochroism, relief and birefringence. Some staurolite grains can be distinguished on the basis of 60° twins, and some allanites by significant extinction angle, length fast orientation, or a dark radiation halo in adjacent hornblende. In addition to this unusual coloring for staurolite and allanite, some kyanite is also distinctly colored in thin sections, with *Z* slightly bluish green, *Y* paler, *X* colorless. Gedrite, hornblende and phlogopite are normally colored. Except for the greater abundance of chlorite, OU 48097 is similar texturally to the quartz-poor bands of OU 48093. Staurolite is very rare.

Chemistry

Microprobe analyses of the staurolite from OU 48093 show the presence of approximately 2% Cr_2O_3 (Table 3). The zinc content is considerable but not unusual, and vanadium and copper are also present as significant traces. Nickel and cobalt were not detected at the 0.2% level. Griffen and Ribbe (1973) and Ribbe (1980) note that traces of Cr_2O^3 (<0.1%) are commonly found in staurolite, and Sharma and MacRae (1981) have recently reported 0.2–0.8% Cr_2O_3 in staurolite from gedrite–cordierite gneisses in northern India, but this appears to be the first record of staurolite with sufficient chromium to affect the color of the mineral.

Comparison of the analyses of chromian staurolite with those of non-chromian staurolites from the same stratigraphic unit reveals an antipathetic relationship between the Al_2O_3 and Cr_2O_3 contents (e.g., analysis 4 in Table 3 is almost identical to analysis 3 except for the virtual absence of Cr_2O_3 in the former and the proportionally higher Al_2O_3). It is concluded that chromium is substituting for aluminum presumably in the octahedral Al sites since, although Al is inferred to be a minor substituent in the tetrahedral Fe site (Smith, 1968; Griffen and Ribbe, 1973), Cr^{3+} is unknown in tetrahedral coordination (Burns and Burns, 1975; Bish, 1977; Phillips et al., 1980).

Controls of chromium content

The range of chromium contents of staurolite and the other phases present in OU 48093 are listed in Table 4. Staurolite is the most chromium-rich mineral present, and the chromium content of the staurolite-bearing bands is considerably greater than that of the staurolite-free bands. That such chromian staurolite has not been reported previously is presumably because of the rarity of chromium-rich rocks sufficiently aluminous to form staurolite. It may also have been overlooked because of its coloring, which mimics common hornblende.

Although the high Cr_2O_3 content of staurolite relative to the other minerals present is conspicuous, staurolite's chromium content is seen to be no more than average when recalculated as atomic Cr/Al (Table 4). This suggests that the large number of appropriate cation sites is the main reason for the high chromium content, rather than any particular "affinity" of staurolite for Cr. A chromium phase is absent, hence these values need not represent saturated Cr contents. A nearby hornblende–cummingtonite rock containing metamorphic Al-chromite, OU 48088, has allanite with up to 4.5% Cr_2O_3 and hornblende with Cr/Al up to 0.10, values about five times higher than in OU 48093.

The chromian staurolite is estimated to have formed at

Table 3. Microprobe analyses of chromian staurolite, OU 48093

	1	2	3	4
SiO_2	28.07	27.34	28.55	28.33
Al_2O_3	52.32	52.38	51.63	54.15
Cr_2O_3	1.78	2.01	1.75	0.04
V_2O_3	0.04	0.08	-	-
CuO	-	0.06	-	-
CaO	0.02	0	0	0
MnO	0.13	0.10	0.15	0.05
MgO	2.79	2.43	3.19	3.36
FeO	11.19	10.70	11.16	11.27
ZnO	0.90	1.05	0.71	0.15
TiO_2	0.75	0.57	0.72	0.57
Total	98.00	96.71	97.86	97.94
	Cations per 46 oxygens			
Si	7.768	7.664	7.897	7.763
Al	17.063	17.308	16.834	17.488
Cr	0.390	0.445	0.383	0.009
V	0.009	0.018	-	-
Cu	-	0.014	-	-
Ca	0.006	0	0	0
Mn	0.031	0.023	0.036	0.012
Mg	1.149	1.014	1.316	1.372
Fe	2.589	2.509	2.582	2.582
Zn	0.184	0.217	0.145	0.030
Ti	0.157	0.120	0.151	0.117
Total	29.34	29.33	29.34	29.37

1, 2, 3 separate crystals of chromian staurolite from OU 48093

4 staurolite from OU 48089

670°C and 8 kbar, from consideration of (1) the anthophyllite–forsterite–magnesite–talc assemblage in a nearby pod of CO_2-metasomatized "metaserpentinite" (Johannes, 1969; Greenwood, 1976), and (2) Fe–Mg partitioning between garnet and biotite (Ferry and Spear, 1978) and Ca partitioning between plagioclase and garnet (Ghent et al., 1979) in adjacent garnet–biotite–kyanite–plagioclase–quartz pelites. The influence of these metamorphic conditions on the chromium content of staurolite is difficult to assess. Seifert and Langer (1970) have shown experimentally that the saturated Cr_2SiO_5 content of kyanite increases markedly with pressure but is relatively insensitive to temperature. Although the structural differences between staurolite and kyanite are undoubtedly significant, staurolite may well behave similarly.

Table 4. Chromium content of minerals in OU 48093

	Weight percent Cr_2O_3 in staurolite-bearing bands	Weight percent Cr_2O_3 in staurolite-free bands	Maximum atomic Cr/Al
staurolite	1.8 - 2.0		0.026
gedrite	0.2 - 0.6	0.02 - 0.4	0.030
hornblende	0.4 - 1.0	0.1 - 0.4	0.044
kyanite	0.4 - 1.1	0.04 - ?	0.012
rutile	1.2	-	
phlogopite	0.7	0.4 - 0.7	0.028
chlorite	0.6	-	0.019
allanite	0.9	-	0.025

Conclusions

Up to 0.45 cations per unit cell of chromium (2 wt.% Cr_2O_3) substitutes for aluminum in staurolite in a mafic metatuff from Fiordland. It is likely that staurolites with higher chromium contents will be found in rocks of higher chromium content, perhaps to the extent that Cr^{3+} would be the dominant cation after Si and Al. The green-dominated pleochroism of chromian staurolite presumably results from the superimposition of a chromium-generated green color on the normal yellow pleochroism of staurolite.

Acknowledgments

I am grateful to J. M. Pillidge for the quality of the polished thin sections he produced, and to Drs. A. F. Cooper, A. Reay and D. S. Coombs for their useful comments on the manuscript.

References

Albee, A. L. (1972) Metamorphism of pelitic schists: reaction relations of chloritoid and staurolite. Geological Society of America Bulletin 83, 3249–3268.

Bence, A. E. and Albee, A. L. (1968) Empirical correction factors for the electron microanalysis of silicates and oxides. Journal of Geology, 76, 382–403.

Bish, D. L. (1977) A spectroscopic and X-ray study of the coordination of Cr^{3+} in chlorites. American Mineralogist, 62, 385–389.

Burns, V. M. and Burns, R. G. (1975) Mineralogy of chromium. Geochimica et Cosmochmica Acta, 39, 903–910.

Čech, F., Povondra, P. and Vrana, S. (1981) Cobaltoan staurolite from Zambia. Bulletin de Minéralogie, 104, 526–529.

Dickson, B. L. and Smith, G. (1976) Low temperature optical absorption and Mössbauer spectra of staurolite and spinel. Canadian Mineralogist, 14, 206–215.

Ferry, J. M. and Spear, F. S. (1978) Experimental calibration of the partitioning of Fe and Mg between biotite and garnet. Contributions to Mineralogy and Petrology, 66, 113–117.

Fleischer, M. (1980) Glossary of Mineral Species, 1980. Mineralogical Record, Tucson, Arizona.

Ghent, E. D., Robbins, D. B. and Stout, M. Z. (1979) Geothermometry, geobarometry, and fluid compositions of metamorphosed calc-silicates and pelites, Mica Creek, British Columbia. American Mineralogist, 64, 874–885.

Gibson, G. M. (1978) Staurolite in amphibolite and hornblendite sheets from the Upper Seaforth River, central Fiordland, New Zealand. Mineralogical Magazine, 42, 153–154.

Greenwood, H. J. (1976) Metamorphism at moderate temperatures and pressures. In D. K. Bailey and R. MacDonald, Eds., The Evolution of the Crystalline Rocks, p. 187–259. Academic Press, London.

Griffen, D. T. (1981) Synthetic Fe/Zn staurolites and the ionic radius of $^{IV}Zn^{2+}$. American Mineralogist, 66, 932–937.

Griffen, D. T., Gosney, T. C. and Phillips, W. R. (1982) The chemical formula of natural staurolite. American Mineralogist, 67, 292–297.

Griffen, D. T. and Ribbe, P. H. (1973) The crystal chemistry of staurolite. American Journal of Science, 273A, 479–495.

Guidotti, C. V. (1970) The mineralogy and petrology of the transition from the lower to upper sillimanite zone in the Oquossoc area, Maine. Journal of Petrology, 11, 277–336.

Hellman, P. L. and Green, T. H. (1979) The high pressure experimental crystallization of staurolite in hydrous mafic compositions. Contributions to Mineralogy and Petrology, 68, 369–377.

Johannes, W. (1969) An experimental investigation of the system MgO–SiO_2–H_2O–CO_2. American Journal of Science, 267, 1083–1104.

Juurinen, A. (1956) Composition and properties of staurolite. Annales Academicae Scientarum Fennicae, Series A, III Geology, 47, 1–53.

Obata, M. and Thompson, A. B. (1981) Amphibole and chlorite in mafic and ultramafic rocks in the lower crust and upper mantle. Contributions to Mineralogy and Petrology, 77, 74–81.

Phillips, T. L., Loveless, J. K. and Bailey, S. W. (1980) Cr^{3+} coordination in chlorites: a structural study of ten chromian chlorites. American Mineralogist, 65, 112–122.

Ribbe, P. H. (1980) Staurolite, In P. H. Ribbe, Ed., MSA Reviews is Mineralogy, v. 6: Orthosilicates. Mineralogical Society of America, Washington, D. C.

Richardson, S. W. (1966) Staurolite. Carnegie Institution of Washington Year Book, 65, 248–252.

Richardson, S. W. (1968) Staurolite stability in part of the system Fe–Al–Si–O–H. Journal of Petrology, 9, 467–489.

Schreyer, W. (1967) A reconnaissance study of the system MgO–Al_2O_3–SiO_2–H_2O at pressures between 10 and 25 kb. Carnegie Institution of Washington Year Book, 66, 382–392.

Schreyer, W. and Seifert, F. (1969) High pressure phases in the system MgO–Al_2O_3–SiO_2–H_2O. American Journal of Science, 267-A, 407–443.

Seifert, F. and Langer, K. (1970) Stability relations of chromian kyanite at high pressures and temperatures. Contributions to Mineralogy and Petrology, 28, 9–18.

Sharma, R. S. and McRae, N. D. (1981) Paragenetic relations in gedrite–cordierite–staurolite–biotite–sillimanite–kyanite gneisses at Ajitpura, Rajasthan, India. Contributions to Mineralogy and Petrology, 78, 48–60.

Skerl, A. C. and Bannister, F. A. (1934) Lusakite, a cobalt-bearing silicate from Northern Rhodesia. Mineralogical Magazine, 23, 598–606.

Smith, J. V. (1968) The crystal structure of staurolite. American Mineralogist, 53, 1139–1155.

Spear, F. S. (1982) Phase equilibria of amphibolites from the Post Pond Volcanics, Mt. Cube quadrangle, Vermont. Journal of Petrology, 23, 383–426.

Streckeisen, A. (1976) To each plutonic rock its proper name. Earth-Science Reviews, 12, 1–33.

von Knorring, O., Sahama, T. G. and Siivola, J. (1979) Zincian staurolite from Uganda. Mineralogical Magazine, 43, 446.

Wells, P. R. A. (1977) Pyroxene thermometry in simple and complex systems. Contributions to Mineralogy and Petrology, 62, 129–139.

Yamaguchi, Y., Akai, J. and Tomita, K. (1978) Chinoamphibole lamellae in diopside of garnet lherzolite from Alpe Arami, Bellinzona, Switzerland. Contributions to Mineralogy and Petrology, 66, 263–270.

Manuscript received, December 28, 1982;
accepted for publication, September 19, 1983.